DOI: https://doi.org/10.33103/uot.ijccce.22.2.10

Optimal Linear Quadratic Control for Knee-Ankle Orthosis System

Fatima I. Alobiady[1], Safanah M. Raafat[2]
[1,2]Control & System Engineering Department, University of Technology, Baghdad, Iraq
[1]cse.19.21@grad.uotechnology.edu.iq, [2]safanah.m.raafat@uotechnology.edu.iq

Abstract— *The control technique for an exoskeleton system for lower limb rehabilitation is complicated, and numerous internal and external elements must be taken into account, in addition to the uncertainties in the system model. In this paper, through the analysis of the lower extremity exoskeleton is utilized to obtain the corresponding equation and its linearized form. The nonlinear differential equations have been linearized by using Jacobean's method in order to facilitate the controller design. Considering the interior and external factors of the connecting rod, the uncertain elements are introduced and therefore the optimal control technique is applied to regulate the system. An optimal state feedback control strategy of Linear Quadratic Regulator (LQR), and LQR-Servo have been implemented in this work. Finally, the physical parameters of the Knee-Ankle Orthosis (KAO) exoskeleton are used, and the simulation results show the advantage and applicability of the proposed controller's design of the Knee-Ankle orthosis system.*

Index Terms— *Rehabilitation, Knee-Ankle orthosis (KAO), Optimal control, LQR-Servo controller.*

I. INTRODUCTION

The main reason for everlasting incapacity global is stroke. Impairments because of stroke caused hemiplegia, making it impossible for patients to engage in activities of daily living. The aid of therapies, like rehabilitation, enables to regain lack abilities. In the previous, the lower limb rehabilitation techniques were fully exercised manually with aid of the therapist to the patients suffering from a stroke [1].

The rehabilitation method includes repetitive exercises that are designed to enhance motor functions. In stroke rehabilitation, the training that facilitates effective recovery should consist of high-intensity and repetitive movements. In the meantime, the patient should be motivated to actively engage in the training over a long period. Conventional training that requires physiotherapists to manually assist the movement of a patient is expensive, labor-intensive, and low repetitive while the duration of the training session is short [2].

The use of robotics can enhance muscular strength and movement in patients with neurological or orthopedic harms particularly stroke rehabilitation [3]. In fact, in many manufactories, manipulators have taken the place of human workers because they own the ability to handle repetitive movements [4]. Integrating robotics into rehabilitation advanced the method of recovery and created the taking walks functionality of the sufferers affected with paraplegic and tetraplegic. Besides, the participation of robotic technology in therapeutic exercises has spread up modern possibilities for surveillance. To help patients perform rehabilitation exercises, assistive robots must be stable and robust enough to

Received 1/October/2021; Accepted 7/November/2021
 ISSN (Print) 1811-9212 ISSN (Online) 2617-3352

DOI: https://doi.org/10.33103/uot.ijccce.22.2.10

support free movement in a limited, repetitive angular pattern. Robustness and stability come with the controller to the robot [1].

Several devices use various control approaches to regulate their systems, and as a result, study into their control has progressed with the advancement of science and technology. It is a fast-developing frontier subject, that is extremely valued by business and academia. The control challenge becomes more significant when we want to track the lower extremity exoskeleton.

The human lower limb system has Multiple Inputs and Multiple Outputs (MIMO), surely complexed within the extreme nonlinear dynamics and uncertainty. The defy matter of unsure systems is the way to transact for them once an actual system has been taking into account. The uncertainty of the system parameters reduces system performance, and system instability is a possibility [5]. These uncertainties have a major impact on the controller, and the overall performance of the model-based controller is strickted by those uncertainties. Therefore, the development of a sensible control algorithm to solve the uncertainty problem of the exoskeletal system of the lower extremities has become an important topic [6].

Meanwhile, some researchers have investigated the optimal control, particularly the Linear Quadratic Regulator (LQR), to achieve a normal movement. In [5] presented the online iterative learning LQR with adaptive iterative learning control is suggested to control trajectory tracking errors for the sake of a leg rehabilitation exoskeleton. In [6] designed the LQR control for exoskeletal systems of the lower extremities taking into account the human 4-DOF gait model in the single support phase. They used the non-dominated sorting genetic algorithm to determine the optimal weighting matrices system dynamics. In [7] used an LQR optimal control to destabilize the lower extremity exoskeleton system. In [8] proposed a robust LQR based Neural-Fuzzy (NF) control scheme is presented in order to overcome the effects of payload uncertainties and external disruption in passive assistance for gait training. Other types of statefeedback controllers as in [9], where H_∞ robust controlller had been designed.

The current paper aims to to improve the performance of an optimal LQR controller by extended it to LQR-Servo controller for the exoskeleton system to minimize the feedback error and ensure the stability of the controlled robotic system.

The paper is structured as follows: Section 2 describes the dynamics model of a KAO system which derived by using Lagrange equations. Section 3 describes the proposed controller design. In Section 4, illustration of simulation results is given. Finally, some Conclusions are drawn in Section 5.

II. MATHEMATICAL MODELING OF KNEE-ANKLE ORTHOSIS (KAO) SYSTEM

A. The dynamics model of Knee-Ankle orthosis system:

The KAO system is a model of 2-DOF exoskeleton. This system introducing using a two-part plane model with revolutionary joints, as shown *in Fig. 1*. It consists of two actuators, one in each joint. This model takes into consideration the flexion/extension of the knee joint and the plantar-flexion/dorsal-flexion of the ankle joint, according to the motions are achieved in a sagittal plane due to the fact exoexercising tasks for lower limbs are the ones of sagittal plane movements [10].

Received 1/October/2021; Accepted 7/November/2021

ISSN (Print) 1811-9212 ISSN (Online) 2617-3352

DOI: https://doi.org/10.33103/uot.ijccce.22.2.10

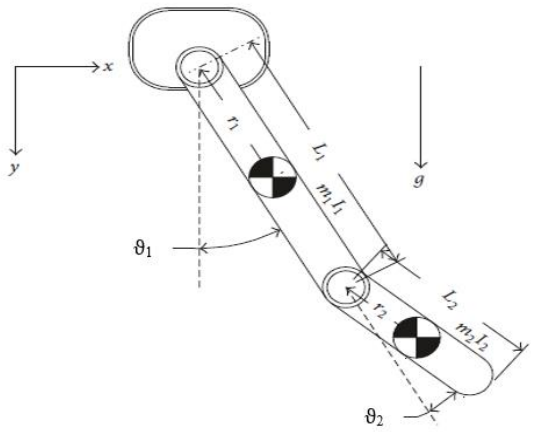

FIG. 1. THE MODEL OF KNEE-ANKLE ORTHOSIS [10].

The Lagrange equations are one of the feasible methods to derive the equations of motion. Accordingly, the Euler-Lagrange equation gives the "generalized" equations of motion as:

$$\frac{d}{dt}\left(\frac{\partial L}{\partial \dot{\theta}_i}\right) - \frac{\partial L}{\partial \theta_i} = \tau_i \text{ , } i = 0, 1, 2, \ldots n \tag{1}$$

where the Lagrangian, L, is obtained from the difference between total kinetic energy, and total potential energy and τ_i corresponding generalized forces. The equation can be expressed as in Eq. (2).

$$L = K_e - V_e \tag{2}$$

where,
$\boldsymbol{K_e}$ is the kinetic energy,
$\boldsymbol{V_e}$ is the potiential energy.

$$\begin{aligned} K_e = {} & \frac{1}{2}m_1 r_1^2 \dot{\theta}_1^2 + \frac{1}{2}I_1 \dot{\theta}_1^2 + \frac{1}{2}I_2 \dot{\theta}_1^2 + \frac{1}{2}I_2 \dot{\theta}_2^2 + \frac{1}{2}m_2 L_1^2 \dot{\theta}_1^2 \\ & + m_2 L_1 r_2 \cos(\theta_2)\, \dot{\theta}_1 \left(\dot{\theta}_1 + \dot{\theta}_2\right) + \frac{1}{2}m_2 {r_2}^2 \left(\dot{\theta}_1 + \dot{\theta}_2\right)^2 \end{aligned} \tag{3}$$

$$V_e = m_1 g r_1 \cos\theta_1 + m_2 g (L_1 \cos\theta_1 + r_2 \cos(\theta_1 + \theta_2)) \tag{4}$$

Using the Lagrange Eq. (2) and the equations (3) and (4), then we get the following:

$$\begin{aligned} L = {} & \frac{1}{2}[m_1 r_1^2 + I_1 + I_2 + m_2 L_1^2]\dot{\theta}_1^2 + \frac{1}{2}I_2 \dot{\theta}_2^2 + m_2 L_1 r_2 \cos(\theta_2)\, \dot{\theta}_1 \left(\dot{\theta}_1 + \dot{\theta}_2\right) \\ & + \frac{1}{2}m_2 {r_2}^2 \left(\dot{\theta}_1 + \dot{\theta}_2\right)^2 - [m_1 r_1 + m_2 L_1] g \cos(\theta_1) - m_2 g r_2 \cos(\theta_1 + \theta_2) \end{aligned} \tag{5}$$

The dynamic model of both human leg and exoskeleton are derived simultaneously, the Lagrange equation supplies a methodical process to procure the dynamics equations of motion for robots.

According to the Lagrange dynamic Eq. (5), the knee and ankle joint moments of τ_1 and τ_2 can be obtained as:

Received 1/October/2021; Accepted 7/November/2021

ISSN (Print) 1811-9212 ISSN (Online) 2617-3352

DOI: https://doi.org/10.33103/uot.ijccce.22.2.10

$$\frac{d}{dt}\left(\frac{\partial L}{\partial \dot{\theta}_1}\right) - \frac{\partial L}{\partial \theta_1} = \tau_1 \tag{6}$$

$$\tau_1 = [m_1 r_1^2 + I_1 + I_2 + m_2 L_1^2 + 2m_2 L_1 r_2\, cos(\theta_2) + m_2 r_2^2]\ddot{\theta}_1 - m_2 L_1 r_2\, sin(\theta_2)\dot{\theta}_2^2$$

$$-2m_2 L_1 r_2\, sin(\theta_2)\dot{\theta}_1\dot{\theta}_2 - [m_1 r_1 + m_2 L_1] g\, sin(\theta_1) - m_2 g r_2\, sin(\theta_1 + \theta_2) \tag{7}$$

$$\frac{d}{dt}\left(\frac{\partial L}{\partial \dot{\theta}_2}\right) - \frac{\partial L}{\partial \theta_2} = \tau_2 \tag{8}$$

$$\tau_2 = [m_2 L_1 r_2\, cos(\theta_2) + m_2 r_2^2]\ddot{\theta}_1 + [I_2 + m_2 r_2^2]\ddot{\theta}_2 - m_2 L_1 r_2\, sin(\theta_2)\, \dot{\theta}_1\dot{\theta}_2$$

$$-m_2 g r_2\, sin(\theta_1 + \theta_2) + m_2 L_1 r_2\, sin(\theta_2)\dot{\theta}_1\, (\dot{\theta}_1 + \dot{\theta}_2) \tag{9}$$

Simplifying equations (7) and (9) yields:

$$\ddot{\theta}_1 = \frac{\alpha_1\tau_1 - \alpha_2\tau_2 + \alpha_3\dot{\theta}_1\dot{\theta}_2 + \alpha_5\dot{\theta}_2^2 + \alpha_6 + \alpha_7 - \alpha_8 + \alpha_9\dot{\theta}_1^2}{\alpha_4} \tag{10}$$

$$\ddot{\theta}_2 = \frac{\beta_1\tau_2 - \beta_2\tau_1 - \beta_3\dot{\theta}_1\dot{\theta}_2 - \beta_5\dot{\theta}_2^2 - \beta_6 + \beta_7 - \beta_8\dot{\theta}_1^2}{\beta_4} \tag{11}$$

where,

$K_1 = m_1 r_1^2 + I_1 + m_2 L_1^2$, $K_2 = m_2 L_1 r_2$, $K_3 = [m_1 r_1 + m_2 L_1] g$,

$K_4 = m_2 g r_2$, $K_5 = m_2 r_2^2$, $K_6 = I_2$,

$s_1 = sin(\theta_1)$, $c_1 = cos(\theta_2)$, $s_{12} = sin(\theta_1 + \theta_2)$, $c_{12} = cos(\theta_1 + \theta_2)$.

$\alpha_1 = [K_5 + K_6]$, $\alpha_2 = (K_2 c_2 + K_5)$, $\alpha_3 = (K_2 K_5 + K_2 K_6) s_2$

$\alpha_4 = [K_5 + K_6][K_1 + 2K_2 c_2 + K_5 + K_6] - \left({K_2}^2 {c_2}^2 + {K_5}^2\right)$, $\alpha_5 = [K_2 K_5 + K_2 K_6] s_2$

$\alpha_6 = [K_3 K_5 + K_3 K_6]\, s_1$, $\alpha_7 = [K_4 K_5 + K_4 K_6] s_{12}$,

$\alpha_8 = (K_2 K_4 c_2 + K_4 K_5) s_{12}$, $\alpha_9 = \left({K_2}^2 c_2 + K_2 K_5\right) s_2$.

$\beta_1 = [K_1 + 2K_2 c_2 + K_5 + K_6]$, $\beta_2 = (K_2 c_2 + K_5)$, $\beta_3 = \left({K_2}^2 c_2 + K_2 K_5\right) s_2$,

$\beta_4 = [K_5 + K_6][K_1 + 2K_2 c_2 + K_5 + K_6] - \left({K_2}^2 {c_2}^2 + {K_5}^2\right)$, $\beta_5 = (K_2^2 c_2 + K_2 K_5) s_2$,

$\beta_6 = (K_2 K_3 c_2 + K_3 K_5)\, s_1$, $\beta_7 = [K_1 K_4 + K_2 K_4 c_2 + K_4 K_6] s_{12}$,

$\beta_8 = \left[K_1 K_2 + 2{K_2}^2 c_2 + K_2 K_5 + K_2 K_6\right] s_2$.

Suppose the state variables of the system are:
$x_1 = \theta_1$: The shank angular position, $x_2 = \theta_2$: The foot angular position.
$x_3 = \dot{\theta}_1$: The shank angular velocity, $x_4 = \dot{\theta}_2$: The foot angular velocity.

So that

Received 1/October/2021; Accepted 7/November/2021
 ISSN (Print) 1811-9212 ISSN (Online) 2617-3352

DOI: https://doi.org/10.33103/uot.ijccce.22.2.10

$$\dot{x}_1 = x_3 , \tag{12}$$

$$\dot{x}_2 = x_4 , \tag{13}$$

$$\dot{x}_3 = \frac{\alpha_1\tau_1 - \alpha_2\tau_2 + \alpha_3 x_3 x_4 + \alpha_5 x_4^2 + \alpha_6 + \alpha_7 - \alpha_8 + \alpha_9 x_3^2}{\alpha_4} \tag{14}$$

$$\dot{x}_4 = \frac{\beta_1\tau_2 - \beta_2\tau_1 - \beta_3 x_4^2 - \beta_5 x_3 x_4 - \beta_6 + \beta_7 - \beta_8 x_3^2}{\beta_4} \tag{15}$$

the outputs are:
$y_1 = \theta_1$: The shank angular position,
$y_2 = \theta_2$: The foot angular position.
the inputs are:
$u_1 = \tau_1$: the external torque at the upper link,
$u_2 = \tau_2$: the external torque at the lower link.

The parameters to be used to develop the KAO system model are as provided in Table I.

TABLE I. LIST OF SYSTEM PARAMETERS [1].

Parameter Name	Symbol	Unit	Value
Shank length	L_1	m	0.2
Foot length	L_2	m	0.08
Shank mass	m_1	Kg	2.8
Foot mass	m_2	Kg	1.17
Shank inertia	I_1	$Kg.m^2$	0.075
Foot inertia	I_2	$Kg.m^2$	0.012
Gravity	g	m/s^2	9.8
$\mathbf{k_n(\tau_d)}$	-	rad	5sin(4πt)

B. Linearized Model of the Knee-Ankle Joint:

By using Jacobean's method, the nonlinear system represented by Eq. (14) and Eq. (15) can be linearized with the equilibrium points listed in Table II. Detailed description of the linearization can be referred to in [11].

TABLE II. THE SYSTEM EQUILIBRIUM POINTS [2].

Equilibrium points	Value	Unit
$\mathbf{x_1}$	0.17	rad
$\boldsymbol{x_2}$	0.35	rad
$\dot{\mathbf{x}}_\mathbf{1}$	0.3	rad\s
$\dot{\mathbf{x}}_\mathbf{2}$	0.4	rad\s
$\boldsymbol{\tau_1}$	0.5	N.m
$\boldsymbol{\tau_2}$	0.5	N.m

The equations could be rewritten as follow:

$$\dot{x}(t) = Ax(t) + Bu(t) \tag{16}$$

$$y\,(t) = Cx(t) + Du(t) \tag{17}$$

Received 1/October/2021; Accepted 7/November/2021
 ISSN (Print) 1811-9212 *ISSN (Online) 2617-3352*

DOI: https://doi.org/10.33103/uot.ijccce.22.2.10

where,
x: is a state vector, $\dot{x}$: is a state differential equation, y: is the output equation, A, B, C, D: are the system nominal matrices which obtained as

$$A = \begin{bmatrix} 0 & 0 & 1.0000 & 0 \\ 0 & 0 & 0 & 1.000 \\ -0.8044 & 1.0560 & 0.0451 & 0.0109 \\ -10.3545 & -710.2931 & -0.3327 & -0.0561 \end{bmatrix}, B = 1.0e+03 * \begin{bmatrix} 0 & 0 \\ 0 & 0 \\ 0.0057 & -0.0080 \\ 0 & 3.9419 \end{bmatrix}$$

$$C = \begin{bmatrix} 0 & 0 & 1 & 0 \\ 0 & 0 & 0 & 1 \end{bmatrix}, D = [0] \quad (18)$$

The parameters of human swing leg system (*i.e.*, support human leg or humanoid robot leg) are given in Table I.

III. CONTROLLER DESIGN

The proposed strategy is an optimal control which can be used to enhance the performance of the system as well as stabilizing it. The main goal of the chosen control is to compute the output control signal which creates balance and guarantees that the supposed purpose (maximizing or decreasing a Performance Index (PI) or a cost function) is achieved for the most dependable and most robust closed-loop system. In this paper, the design of "LQR optimal control algorithm" and LQR-servo controller are developed.

A. LQR Optimal Controller:

The LQR controller is an effective method applied to control linearized within the state-space domain [12], as can be seen in in *Fig. 2*. The LQR controller offers stability securing, performance, and robustness in a closed control loop in the presence of uncertainty in the system [13]. The proposed LQR controller aims to determine the state-feedback control vector ***K***, which gives control vector ***u***. Moreover, the law of linear state feedback control shows in Eq. (19), that it attained through minimizing a quadratic cost function shown in Eq. (20). Then, the Algebraic Riccati equation gives the Riccati solution, ***P*** as expressed in Eq. (21), [14-15].

$$u(t) = -Kx(t) = -R^{-1}B^{T}Px(t) \quad (19)$$

$$J = \int_0^{\infty} [x^{T}(t)Qx(t) + u^{T}(t)Ru(t)]dt \quad (20)$$

$$A^{T}P + AP - PBR^{-1}B^{T}P + Q = 0 \quad (21)$$

where,
Q: is positive definite weight matrix
R: is positive semi-definite weight factor.

The ***Q*** and ***R*** are selected with suitable weightings for the state of the system., $x = \left[\theta_1 \ \theta_2 \ \dot{\theta}_1 \ \dot{\theta}_2\right]^{T}$ to create the LQR controller supported on the reduction of quadratic performance index, **J**.

Received 1/October/2021; Accepted 7/November/2021

ISSN (Print) 1811-9212 *ISSN (Online) 2617-3352*

DOI: https://doi.org/10.33103/uot.ijccce.22.2.10

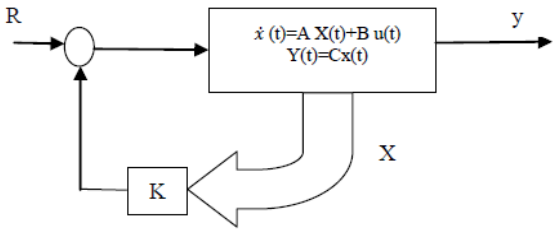

FIG. 2. FULL STATE FEEDBACK REPRESENTATION OF KNEE-ANKLE ORTHOSIS.

B. Linear Quadratic Regulator Servo (LQR-Servo) Optimal Control:

The LQR control provides quite good activity for regulation responsibilities, however, it is incapable to ensure the pursuance of dynamic references due to the lack of integrated methods in the controller [16]. The latter is added using an LQR-servo method of control, as shown in *Fig. 3*. The LQ-servo is an idealistic state feedback controller which could keep tracking of the dynamic reference and remove the error because of the effect of the integral term [17]. This is performed through enhancing the state of system through the output error integration shown in the LQR-Servo controller structure below.

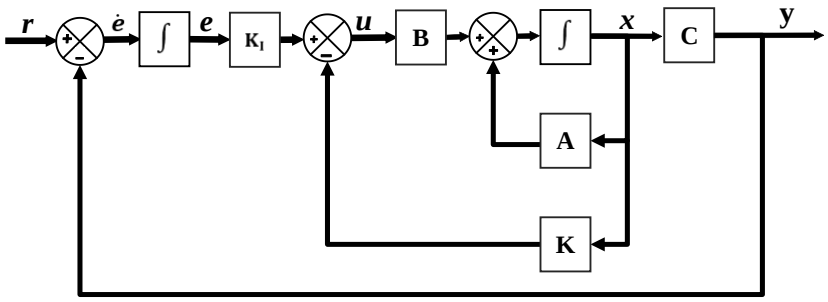

FIG. 3. TYPICAL IMPLEMENTATION OF THE LQR SERVO.

The error vector could be written as follow:

$$\dot{e} = r - y = r - Cx \tag{22}$$

where ***r*** is the reference signals.

The state space is a description of the specified system as shown below:

$$\dot{x}_E = A_E\, x_E + B_E\, u + r \tag{23}$$

Let:

$$A_E = \begin{bmatrix} A & 0_{4,2} \\ -C & 0_{2,2} \end{bmatrix}, B_E = \begin{bmatrix} B \\ 0_{2,2} \end{bmatrix},$$

$$C_E = [C \quad 0], D_E = [D] \tag{24}$$

The new state vector, $x_E = [x \quad e]^T$

$$\begin{bmatrix} \dot{x} \\ \dot{e} \end{bmatrix} = \begin{bmatrix} A & 0_{4,2} \\ -C & 0_{2,2} \end{bmatrix} \begin{bmatrix} x \\ e \end{bmatrix} + \begin{bmatrix} B \\ 0_{2,2} \end{bmatrix} \times u + \begin{bmatrix} 0_{4,2} \\ 1_{2,2} \end{bmatrix} \times r \tag{25}$$

where,

Received 1/October/2021; Accepted 7/November/2021

ISSN (Print) 1811-9212 ISSN (Online) 2617-3352

DOI: https://doi.org/10.33103/uot.ijccce.22.2.10

A_E : The augmented system matrix, B_E : The augmented input matrix, x_E: The augmented of state vectors, both A_E and B_E augmented controllable pair of system matrices.

Now, the control input $\boldsymbol{u}$ is obtained from the augmented system illustration from as following:

$$x_I = [\int (x_{r1} - x_1) \quad \int (x_{r2} - x_2)]^T \tag{26}$$

$$x_E = \begin{bmatrix} \theta_1 & \theta_2 & \dot{\theta}_1 & \dot{\theta}_2 & x_I \end{bmatrix}^T \tag{27}$$

$$u = -K_E \times x_E = -[K \quad K_I] \begin{bmatrix} x \\ x_I \end{bmatrix} \tag{28}$$

where, x_r: is unmeasured states, K_E: is the control gains, which is calculated by using the ***lqr*** command in MATLAB using the linear model matrices.

IV. SIMULATION RESULTS

This part of the paper includes the results obtained by MATLAB. The impact of optimal control relies upon the choice of weight matrices (***Q*** & ***R)***. Broadly, the weight matrices (***Q*** & ***R***), if they are not properly selected, the result could not reach the performance requirements. So, after getting an appropriate (***Q*** & ***R)***, the optimal gain matrix ***K*** can be calculated. In the following, the simulation results will be illustrated.

A. LQR:

By the application of Eqs. 19-21 using MATAB, and selecting the weight matrix as follow:

$$Q = \begin{bmatrix} 500 & 0 & 0 & 0 \\ 0 & 500 & 0 & 0 \\ 0 & 0 & 500 & 0 \\ 0 & 0 & 0 & 500 \end{bmatrix} \text{ and } R = \begin{bmatrix} 0.01 & 0 \\ 0 & 0.01 \end{bmatrix}.$$

The initial state $x_0 = [0.5; 0.5; 0.5; 0.5]$. The feedback gain $\boldsymbol{K_{lqr}}$ is obtained as follows:

$$K_{lqr} = \begin{bmatrix} 1.2147e^{+2} & -3.7532e^{+1} & 3.1100e^{+2} & 5.9136e^{-1} \\ 5.0022 & 1.1336e^{+2} & -2.7493e^{+1} & 2.2367e^{+2} \end{bmatrix}$$

The resulted closed-loop response of the system using the LQR Controller is shown in *Fig. 4*, and the control signal is shown in *Fig.* 5. It is clear that although the resulting control signal needs to be concentrated within certain accepted values, the LQR control can effectively regulate the system. *Fig*. 6 shows the error in this case, where the reference signal is considered as zero. In order to track a change in the reference signal the LQR needs to be enhanced by adding the integral of the errors, as will be described next.

Received 1/October/2021; Accepted 7/November/2021

ISSN (Print) 1811-9212 ISSN (Online) 2617-3352

DOI: https://doi.org/10.33103/uot.ijccce.22.2.10

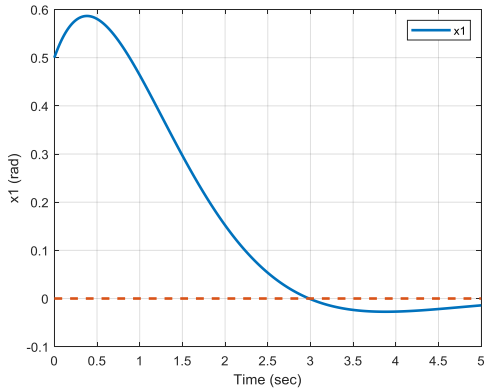

(a) The first state x_1

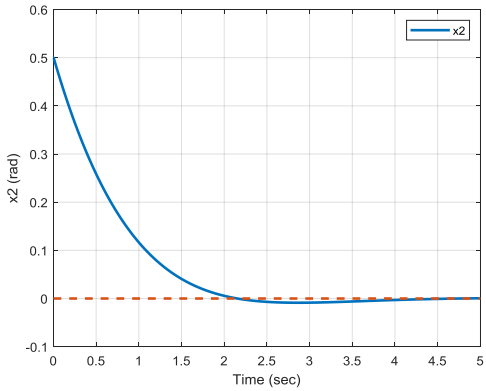

(b) The second state x_2

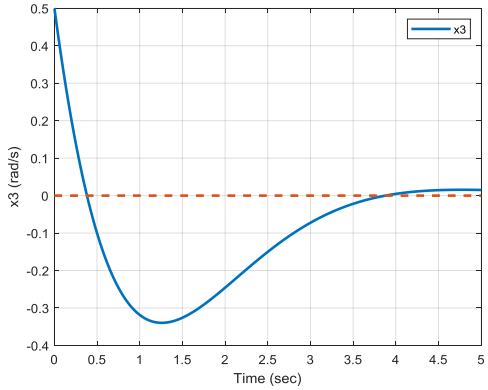

(d) the thrid state x_3

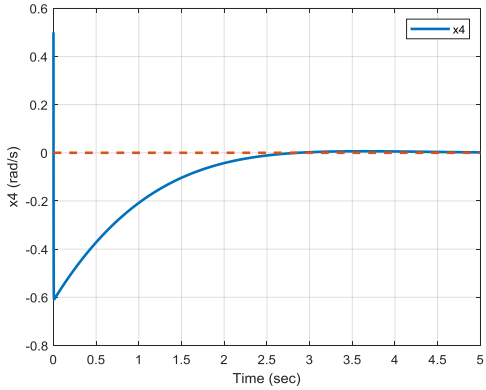

(c) the fourth state x_4

FIG. 4. A CLOSED LOOP RESPONSE USING LQR CONTROLLER.

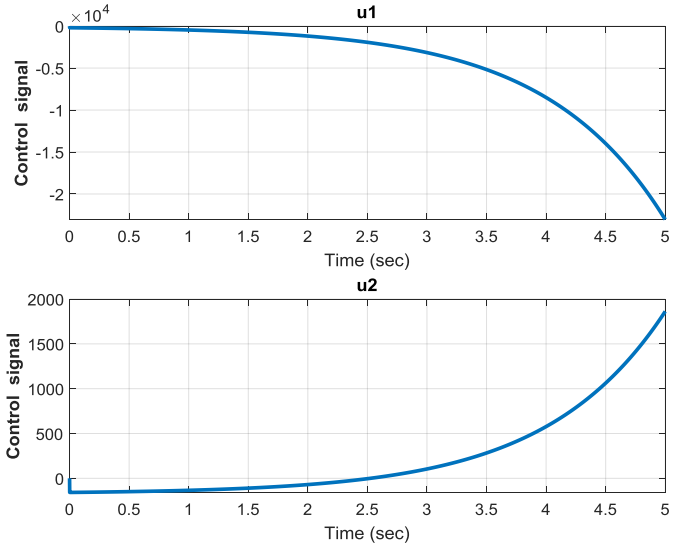

FIG. 5. THE CONTROL SIGNALS.

Received 1/October/2021; Accepted 7/November/2021

ISSN (Print) 1811-9212 *ISSN (Online) 2617-3352*

DOI: https://doi.org/10.33103/uot.ijccce.22.2.10

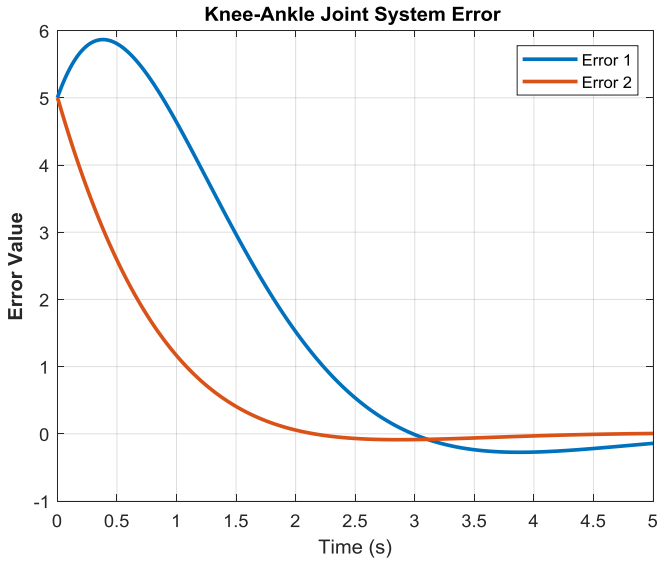

FIG. 6. THE ERROR SIGNALS USING LQR CONTROL.

B. LQR-servo:

By using the approach that is described in Section III.B and using the following weight matrices:

$$Q = 0.2 * ([C_E' * C_E]), \text{ and } R = 5 * [1 \quad 0.1 ; 0 \quad 1],$$

and initial state $x_0 = [-0.2 ; -0.8 ; 5 ; 1 ; 0 ; 0]$, the following controller gain K_{lqr} has been obtained:

$$K_{lqr} = \begin{bmatrix} -1.1461e^{-1} & -6.2649e^{-2} & 8.1863e^{-1} & 1.5265e^{-4} & -1.9871 & 3.9176e^{-2} \\ 2.1089e^{-3} & -1.4160e^{-1} & -2.8218e^{-2} & 3.0485e^{-2} & 6.5794e^{-2} & -1.9823 \end{bmatrix}$$

The applied reference signals for both joints are taken to be ref = 4 rad.

The KAO-controlled system has efficiently tracked the reference signal. In addition, the obtained results using the LQR-Servo controller eliminate the steady-state tracking error minimizes the overshoot and the oscillation of the system response in the time domain as obtained in figures below.

Fig. 7 contains a closed-loop response of the system applying LQR-servo control, which shows the behavior of the LQR-servo controller in tracking the reference signals, and *Fig.* 8 displays the control input signal *u*, which is much improved than that in the LQR case that shown in *Fig.* 6, and *Fig.* 9 shows the resulting error signal. It is clear that the error signals were reduced to zero as required.

Received 1/October/2021; Accepted 7/November/2021

ISSN (Print) 1811-9212 ISSN (Online) 2617-3352

DOI: https://doi.org/10.33103/uot.ijccce.22.2.10

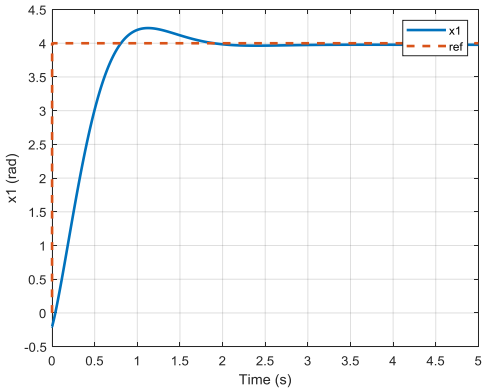

(a) The first state x_1

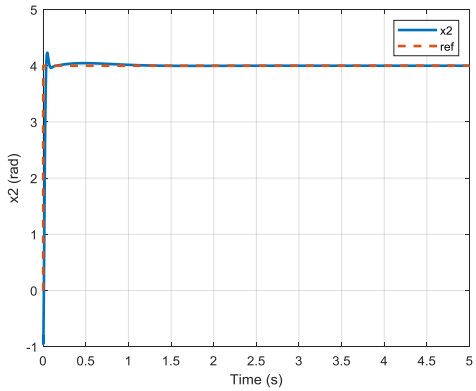

(b) The second state x_2

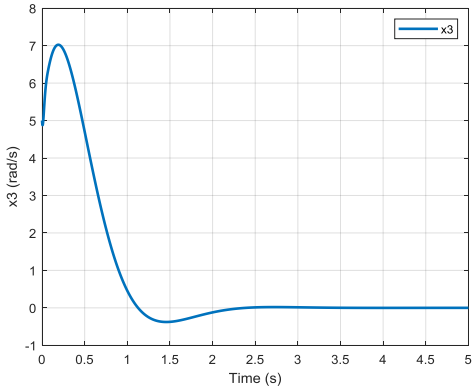

(c) The third state x_3

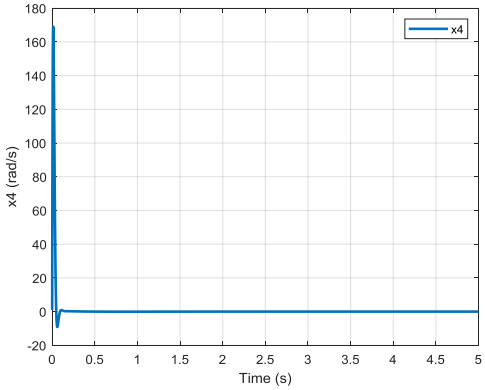

(d) The fourth state

FIG. 7. A CLOSED LOOP RESPONSE USING LQR-SERVO CONTROLLER.

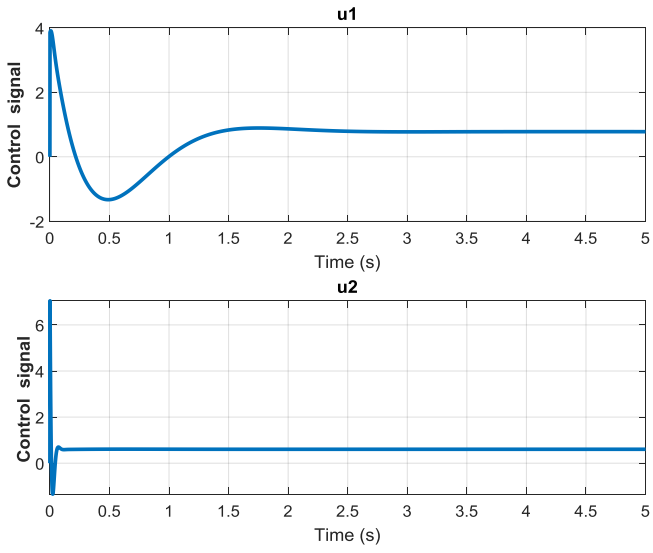

FIG. 8. THE CONTROL SIGNALS.

Received 1/October/2021; Accepted 7/November/2021

ISSN (Print) 1811-9212 *ISSN (Online) 2617-3352*

DOI: https://doi.org/10.33103/uot.ijccce.22.2.10

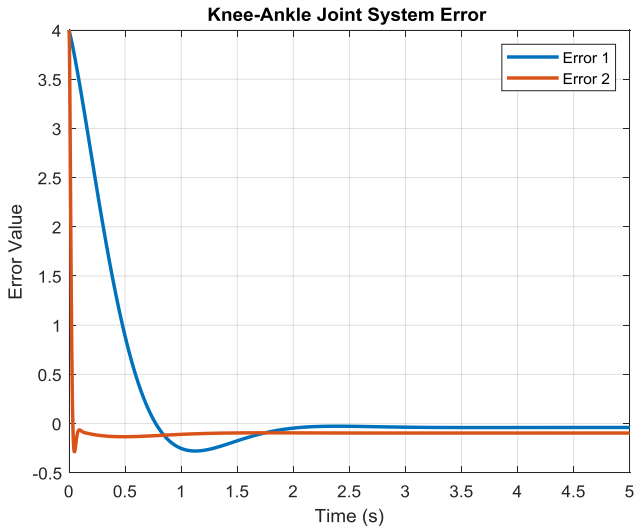

FIG. 9. THE ERROR SIGNALS.

To further examine the robustness of the proposed LQR-Servo control, an external sudden disturbance of 0.4 rad is applied to the KAO system at time = 2 *sec*, as shown in *Fig. 10*. It may be noticed that the developed LQR-Servo controller can effectively reject the external disturbance and maintain the robustness of the KAO controlled system. *Fig. 11* displays the control input signal *u*, which shows the signal has defeated the sudden disturbance and be stable. *Fig. 12* shows the effecting error signal.

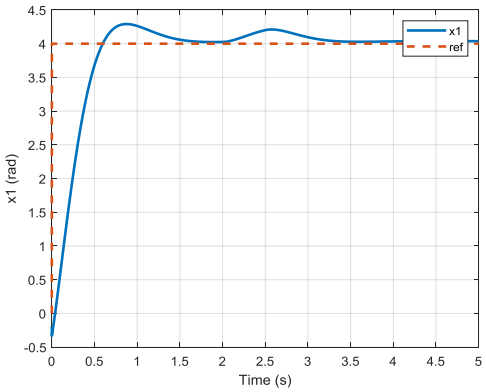

(a) The first state x_1.

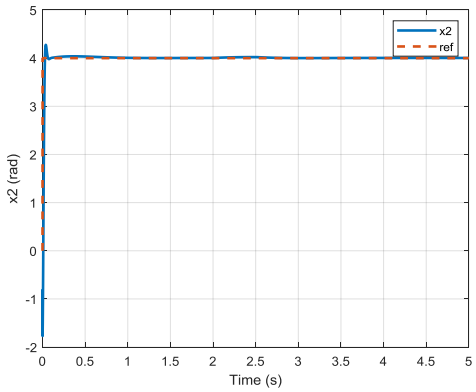

(b) The second state x_2.

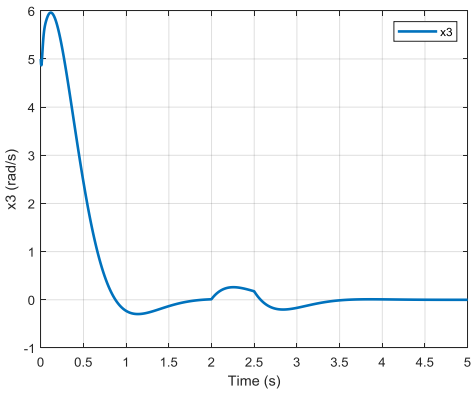

(c) The third state x_3.

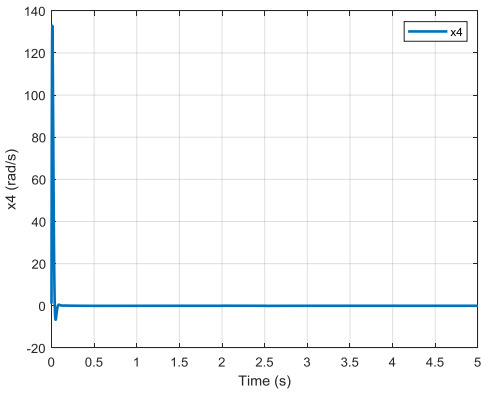

(d) The fourth state x_4.

FIG.10. A CLOSED LOOP RESPONSE USING LQR-SERVO CONTROLLER WITH DISTURBANCE INPUT.

Received 1/October/2021; Accepted 7/November/2021

ISSN (Print) 1811-9212 *ISSN (Online) 2617-3352*

DOI: https://doi.org/10.33103/uot.ijccce.22.2.10

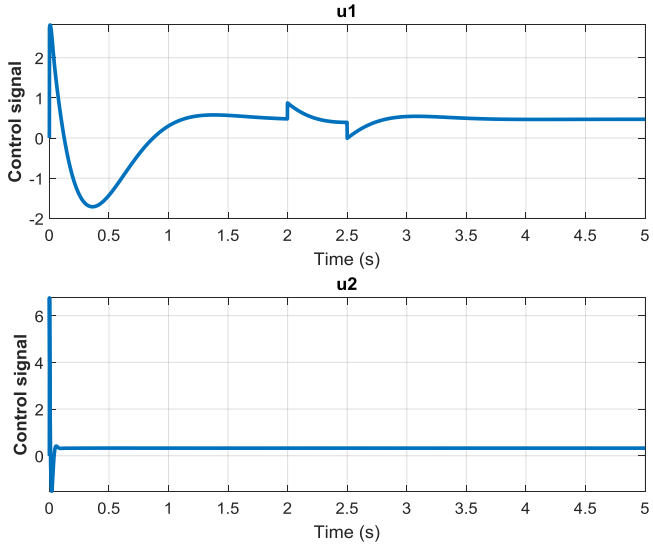

FIG. 11. THE CONTROL SIGNALS.

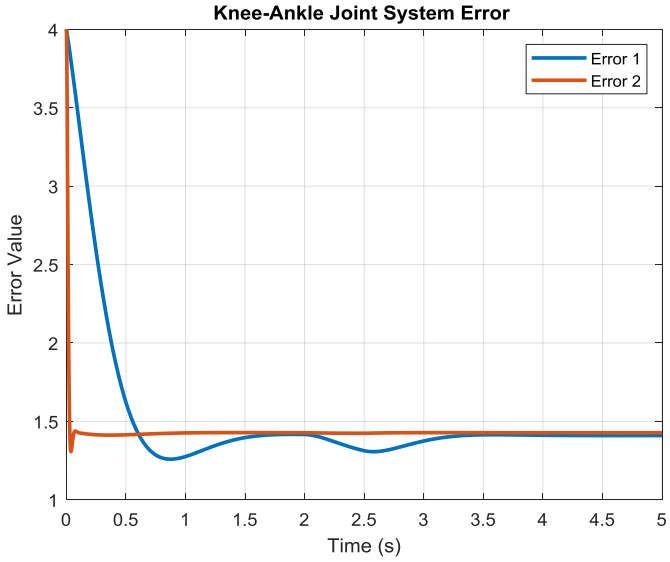

FIG. 12. THE ERROR SIGNALS.

Another test has been investigated by considering the effects of noise on the system. Although the effect of the noise can be noticed in the control signal, where the disturbance is mainly affecting, the controlled system can still maintain the robustness of stability and performance. The resulted response is as shown in *Fig. 13*, while *Fig. 14* shows the noise effect with the control signal *u*. *Fig. 15* shows the resulting error signal. It can be observed that the KAO-controlled system can still maintain robustness and stability.

Received 1/October/2021; Accepted 7/November/2021

ISSN (Print) 1811-9212 *ISSN (Online) 2617-3352*

DOI: https://doi.org/10.33103/uot.ijccce.22.2.10

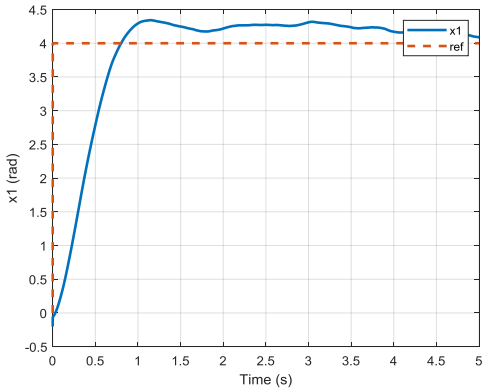

(a) The first state x_1.

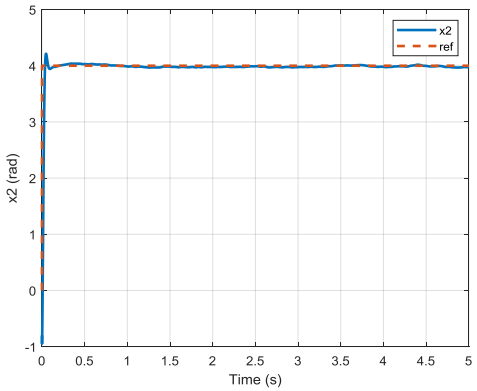

(b) The second state x_2.

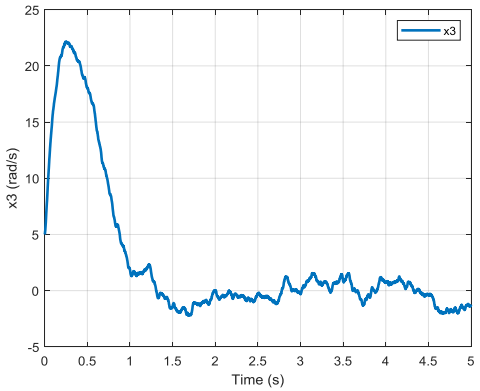

(c) The third state x_3.

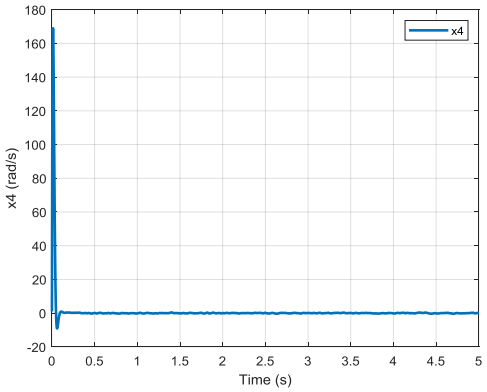

(d) The fourth state x_4.

FIG. 13. A CLOSED LOOP RESPONSE USING LQR-SERVO CONTROLLER WITH NOISE INPUT.

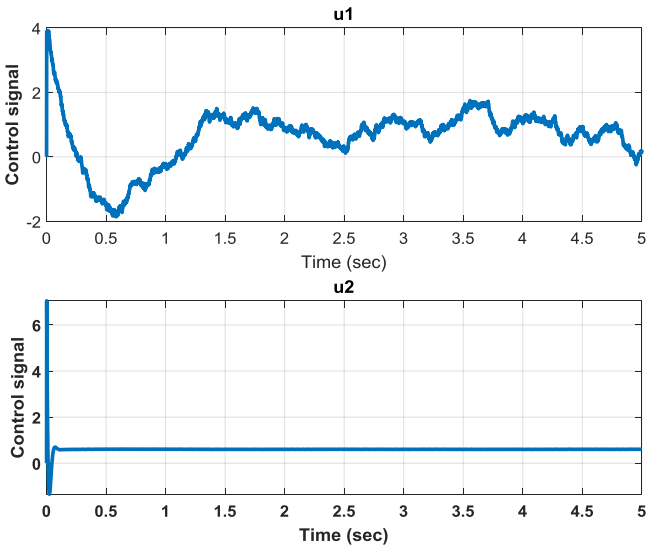

FIG. 14. THE CONTROL SIGNALS.

Received 1/October/2021; Accepted 7/November/2021

ISSN (Print) 1811-9212 *ISSN (Online) 2617-3352*

DOI: https://doi.org/10.33103/uot.ijccce.22.2.10

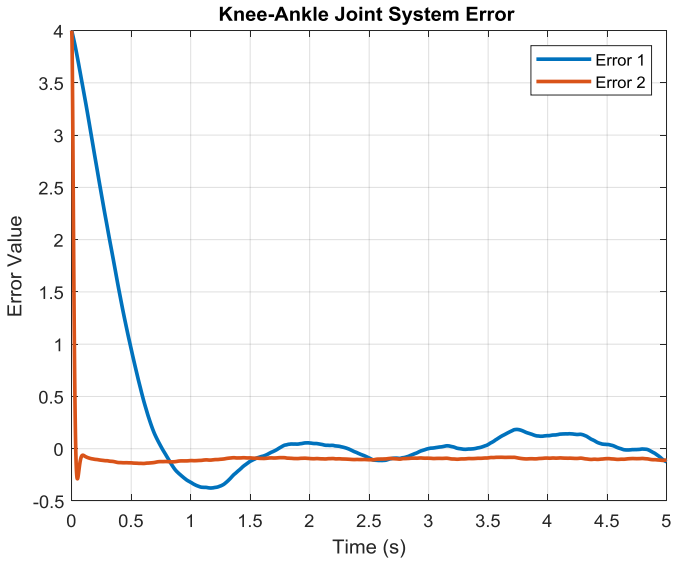

FIG. 15. THE ERROR SIGNALS.

The integral action within the suggested LQR-servo controller has considerably reduces the steady-state error. This approach does not only achieve a smooth stabilization curve with the least amount of overshoot and oscillation of angle and distance. Also, it achieves the LQR controller resilience with tracking performance.

V. CONCLUSIONS

In this paper, the non-linear model of the KAO system is linearized, and then a linear optimal controller has been applied effectively to the system. The implemented LQR optimal control approach shows good stability performance. The performance weight matrices (***Q*** and ***R*****)** have been calculated, so the position angles of the robot meet the required time domain characteristics in the regulatory mode of operation. Then, the LQR-servo control method has been applied to the KAO system. The tracking performance has been achieved in this case, even with the presence of disturbance.

The next step of this work will be to enhance the performance of the controlled system by using optimization to improve and selection of ***Q*** and ***R*** values of the optimal controller and by considering the nonlinear system's model and upgrade the controller to include the nonlinearities of the system using the computed torque approach.

REFERENCES

[1] S. F. Ahmed *et al.*, "Robotic exoskeleton control for lower limb rehabilitation of knee joint," *Int. J. Eng. Technol.*, vol. 7, no. 2, pp. 56–59, 2018.

[2] V. Sangveraphunsiri, "Mechanical Power to Identify Human Performance for a Lower Limb Rehabilitation Robot," *Eng. J.*, vol. 23, no. 4, pp. 91–105, 2019.

[3] A. Sutapun and V. Sangveraphunsiri, "A Novel Design and Implementation of a 4-DOF Upper Limb Exoskeleton for Stroke Rehabilitation with Active Assistive Control Strategy," *Eng. J.*, vol. 21, no. 7, pp. 275–291, 2017.

[4] A. T. Phan, H. N. Thai, C. K. Nguyen, Q. U. Ngo, H. A. Duong, and Q. T. Vo, "Trajectory Tracking Control Design for Dual-arm Robots using Dynamic Surface Controller," *Eng. J.*, vol. 24, no. 3, pp. 159–168, 2020.

[5] N. Ajjanaromvat and M. Parnichkun, "Trajectory Tracking Using Online Learning LQR with Adaptive Learning Control of a Leg-Exoskeleton for Disorder Gait Rehabilitation," *Mechatronics*, vol. 51, no. September 2017, pp. 85–96, 2018.

Received 1/October/2021; Accepted 7/November/2021

ISSN (Print) 1811-9212 ISSN (Online) 2617-3352

DOI: https://doi.org/10.33103/uot.ijccce.22.2.10

[6] J. Gupta, R. Datta, A. K. Sharma, A. Segev, and B. Bhattacharya, "Evolutionary Computation for Optimal LQR Weighting Matrices for Lower Limb Exoskeleton Feedback Control," *Proc. - 22nd IEEE Int. Conf. Comput. Sci. Eng. 17th IEEE Int. Conf. Embed. Ubiquitous Comput. CSE/EUC 2019*, pp. 24–29, 2019.

[7] J. Chen, Y. Fan, M. Sheng, and M. Zhu, "Optimized Control for Exoskeleton for Lower Limb Rehabilitation with Uncertainty," *Proc. 31st Chinese Control Decis. Conf. CCDC 2019*, no. 2, pp. 5121–5125, 2019.

[8] J. Narayan and S. K. Dwivedy, "Robust LQR-Based Neural-Fuzzy Tracking Control for a Lower Limb Exoskeleton System with Parametric Uncertainties and External Disturbances," *Appl. Bionics Biomech.*, vol. 2021, 2021.

[9] Hazem I. Ali, "H-infinity Based Full State Feedback Controller Design for Human Swing Leg," Engineering and Technology Journal, vol. 36, no. 3, Mar. 2018.

[10] M. O. Ajayi, K. Djouani, and Y. Hamam, "Bounded Control of an Actuated Lower-Limb Exoskeleton," *J. Robot.*, vol. 2017, 2017.

[11] H. I. Ali, A. F. Hasan, and H. M. Jassim, "Optimal H2PID Controller Design for Human Swing Leg System Using Cultural Algorithm," *J. Eng. Sci. Technol.*, vol. 15, no. 4, pp. 2270–2288, 2020.

[12] K. Ogata, "Modern control engineering," Vol. 5. Upper Saddle River, NJ: Prentice hall, 2010.

[13] T. Teng Fong, Z. Jamaludin, A. Y. Bani Hashim, and M. A. A. Rahman, "Design and Analysis of Linear Quadratic Regulator for a Non-Linear Positioning System," *Appl. Mech. Mater.*, vol. 761, pp. 227–232, 2015.

[14] L. T. Rasheed, "Optimal Tuning of Linear Quadratic Regulator Controller Using Ant Colony Optimization Algorithm for Position Control of a Permanent Magnet DC Motor," *IRAQI JOURNAL OF COMPUTERS, COMMUNICATIONS, CONTROL AND SYSTEMS ENGINEERING*, pp. 29–41, Jul. 2020.

[15] B. F. Midhat, "Optimal LQR Controller Design for Wing Rock Motion Control in Delta wing Aircraft," *Engineering and Technology Journal*, 2017.

[16] B. K. Abd-Al Amear, S. M. Raafat, and A. Al-Khazraji, "Glucose Controller for Artificial Pancreas," *2019 Int. Conf. Innov. Intell. Informatics, Comput. Technol. 3ICT 2019*, no. September, pp. 1–6, 2019.

[17] S. M. Raafat, B. K. Abd-AL Amear, and A. Al-Khazraji, "Multiple Model Adaptive Postprandial Glucose Control of Type 1 Diabetes," *Eng. Sci. Technol. an Int. J.*, vol. 24, no. 1, pp. 83–91, 2021.

Received 1/October/2021; Accepted 7/November/2021
 ISSN (Print) 1811-9212 *ISSN (Online) 2617-3352*